JOURNAL OF PROPULSION AND POWER
Vol. 21, No. 1, January–February 2005

Improvement on the Scaling Theory of the Stationary Plasma Thruster

Yu Daren,* Ding Yongjie,† and Zeng Zhi‡
Harbin Institute of Technology, 150001 Heilongjiang, People's Republic of China

The scaling theory of the stationary plasma thruster provides a basis for the design of thrusters. We first briefly discusses the disadvantages of the existing scaling theory, and then we improve it by introducing a scaling index variable. If the scaling index variable is properly set, the thruster performance prediction is much improved, and the model can be used to identify areas for design improvement. For example, for lower powers the probability of magnetic saturation can be reduced, and ion sputtering can be alleviated; for higher powers the power-to-weight ratio and thrust-to-weight ratio can be improved.

Nomenclature

B_i = magnetic field induction in magnetic core
B_r = magnetic field induction in channel
B_s = saturation magnetic field induction in magnetic core
E = electron field
e = electron charge
g = acceleration of gravity
g_i = volumetric rate of ionization
I = discharge current
j_d = discharge current density
j_e = electron current density
j_{ee} = electron current density at exist of ionization-acceleration region
j_{ie} = ion current density at exist of ionization-acceleration region
L = axial characteristic length
l = length of channel
M = ion and atom mass
M_t = thruster mass
m = electron mass
$\dot{m}$ = mass flow rate
n = particle density
P = power
P^* = power of the desired thruster
R_i = iron core radius
r, R = inner and outer radius of channel
r_e = electron Larmor radius
T = thrust
T_e = electron temperature
T_n = neutral particle temperature
U_d = discharge voltage
u_d = electron drift velocity
u_{et} = electron thermal velocity
u_{ez} = electron axial velocity
u_{ie} = ion exhaust velocity
u_{ne} = neutral exhaust velocity
W = channel width
z = axial coordinates
α = ionization degree
α_i = electron impact ionization rate
β = hall parameter
ζ = scaling index variable
λ = mean free path
μ_{e0} = electron mobility in the absence of magnetic field
$\mu_{e\perp}$ = electron mobility across magnetic field
ν_e = total electron collisions frequency
ν_{ea} = electron collision frequency with atoms
ν_{ei} = electron collision frequency with ions
ν_{ew} = electron collision frequency with wall
ν_i = ionizational electron collision frequency
σ = collision cross section
σ_0 = classical plasma conductivity
$\sigma_\perp$ = conductivity across magnetic field
Φ = magnetic flux

Subscripts

e = electron density
i = ion density
ie = ion density near exist
n = neutral particle density
ne = neutral density near exist
1, 2 = parameters of the thruster designed according to the existing scaling theory and our proposed one respectively

Received 18 October 2003; revision received 17 August 2004; accepted for publication 12 September 2004.

*Professor, School of Energy Science and Engineering; yudaren@hcms.hit.edu.cn.
†Ph.D. Student, School of Energy Science and Engineering; dingyongjie@hcms.hit.edu.cn.
‡Master Student, School of Energy Science and Engineering; zengzhi@hcms.hit.edu.cn.

I. Introduction

BECAUSE of their high specific impulse and high thrust efficiency, stationary plasma thrusters (SPT) are useful for many on-orbit applications including stationkeeping, orbit rephasing, and orbit transfer.[1] The flight heritage and unique performance characteristics of SPT result in the possibility of reduced launch mass and longer time in station.[2]

Current SPT research has concentrated primarily on 1-kW class thrusters because they have been of primary interest for commercial and military satellite uses. However, as indicated by industry trends and integrated high payoff rocket propulsion technology (IHPRPT) goals, the SPT market is expanding beyond the 1-kW class thruster to both lower powers for small satellites and higher powers for orbit transfer missions.[3] This evolution in SPT power level leads to the development of the SPT scaling theory.

In the existing scaling theory,[4–12] global geometric similarity ($W/L = \text{const}$, $R/L = \text{const}$) is adopted, which restricts the degrees of freedom in the thruster design. A number of issues arise as a result of the simple linear scaling of the overall thruster dimensions. First, in scaling to lower powers, B_r is inversely proportional to P because $R/L = \text{const}$. At lower powers, this can result in magnetic

core saturation, which precludes magnetic field optimization and results in low efficiency.[4] Moreover, if global geometric similarity is adopted when designing lower powers the channel width will be proportional to the power, leading to serious ion sputtering that will shorten thruster's lifetime.[5,6] Second, in scaling to higher powers, the rate of the power increase will be far smaller than that of the thruster weight when $R/L = \text{const}$, leading to lower $P/M_t g$ and $T/M_t g$. These results show that the thrusters designed according to the existing scaling theory cannot satisfy the demands of the orbit transfer or deep-space exploration. Last, according to the existing scaling theory $\dot{m}$, P and T are proportional to R, which disagrees with the experimental results.[7] Shown in Figs. 1–3 are plots of experimental design points showing the dependence of power, mass flow rate, and thrust on SPT radius along with the prediction of the existing scaling theory. The data are also summarized in Table 1 (Ref. 7).

It is obvious that great differences exist between the results obtained from the existing scaling theory and experimental results. The preceding analyses show that it is necessary to improve the existing theory for the design of thrusters.

Table 1 SPT parameters

Parameter	SPT-35	SPT-50	SPT-60	SPT-70	SPT-100
Diameter, mm	35	50	60	70	100
Mass flow rate, mg/s	0.9	1.6	2.2	2.5	5.5
Thrust, mN	10	20	30	40	83
Specific impulse, s	1200	1250	1400	1570	1600
Power, kW	0.2	0.35	0.517	0.593	1.35
Efficiency, %	30	35	40	50	50

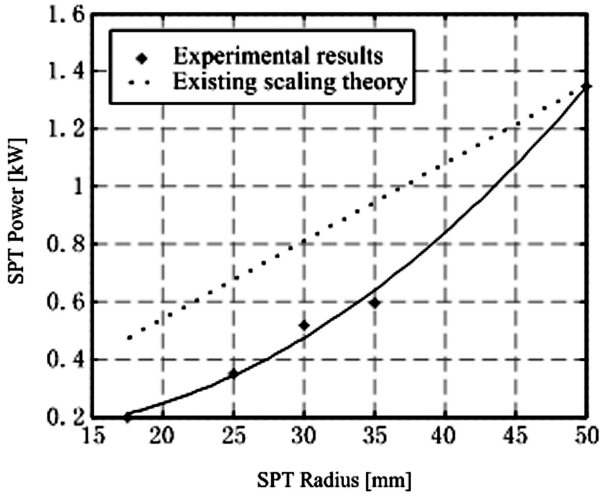

Fig. 1 Relationship between P and R.

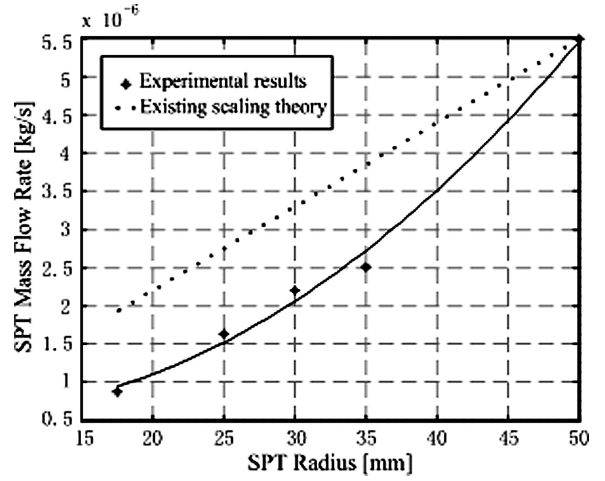

Fig. 2 Relationship between $\dot{m}$ and R.

II. Overview of the Scaling Theory

SPT scaling has been the subject of considerable research: Bugrova et al. studied the relationship between the particle mean free path and the characteristic length and then obtained the similarity criterion in 1974 (Refs. 8 and 9). They also studied the similarity criterion for other propellant.[10,11] To preserve the specific impulse and efficiency, Khayms and Martinez-Sanchez[5] and Hargus and Cappelli[12] proposed the existing scaling theory based on the following assumptions:

1) The average electron energy, or electron temperature, must be conserved, which means $T_e(z/L)$ should be conserved; this quantity is critical to the ionization process and is a characteristic of the propellant used.[13]

2) $U_d = \text{const}$ (Ref. 13).

3) $\lambda/L = \text{const}$ (Ref. 5).

4) Global geometric similarity ($W/L = \text{const}$ and $R/L = \text{const}$) (Ref. 14).

As shown in Table 1, the specific impulse and efficiency are not invariant. The efficiencies of SPT35 and SPT100 are 30 and 50%, respectively, which can be caused by the losses from ion sputtering and ionization process. Research on loss mechanism is still going on.

The resulting relationships are shown in Table 2.

Using their scaling theory and data from the SPT100, Khayms and Martinez-Sanchez designed a 50-W mini-SPT with outer diameter of 3.7 mm (Ref. 5). The thruster had an efficiency of 6%, too low to be of value. Additionally, the thruster was too small to be manufactured. The experimental magnetic field induction was only about 0.17–0.25 T, lower than the desired 0.4–0.5 T. These results show the need for an improved scaling theory.

Table 2 Parameter relationships in the existing scaling theory

Parameters	Relationship
n	$\sim R^{-1}$
$\dot{m}$	$\sim R$
P	$\sim R$
I	$\sim R$
j_d	$\sim R^{-1}$
B_r	$\sim R^{-1}$
E	$\sim R^{-1}$
u_d	const
ω_e	$\sim R^{-1}$
r_e	$\sim R$
$\mu_{e\perp}$	$\sim R$
T	$\sim R$

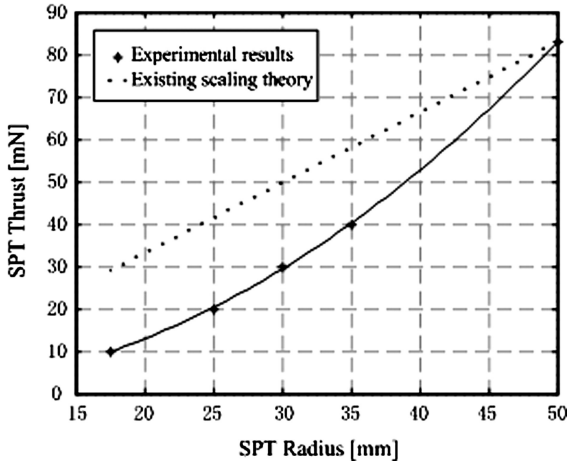

Fig. 3 Relationship between T and R.

III. Improvement on the Existing Scaling Theory

A simple linear scaling of overall thruster dimensions results in serious ion sputtering for lower powers and low power-to-weight ratio for higher powers. To alleviate these problems, the modification $R^{2-\zeta}/L = \text{const}$ is adopted in our proposed scaling theory. The characteristic dimensions are redefined to include not only the length, but also the width of the characteristic region (ionization-acceleration region). Then we study the relationships between characteristic dimensions and other parameters.

A. Assumptions of Our Proposed Scaling Theory

Our proposed scaling theory is established on the following assumptions:

1) $T_e(z/L) = \text{const}$.
2) $U_d = \text{const}$.
3) $\lambda/L = \text{const}$.
4) Local geometric similarity is shown by $r/R = \text{const}$ and $R^{2-\zeta}/L = \text{const}$. ζ equals 1 in the existing scaling theory.

The assumption of invariant electron temperature is justified if the ratio of power dissipated to electrons is proportional to electron energy loss at the wall, which is probably the dominant energy loss mechanism.[12,13] For constant specific impulse, the desired discharge voltage, a design parameter, should be specified as the same as that of the model. λ/L has to be kept constant so that SPT can operate under the ionization process similarity condition. $R^{2-\zeta}/L = \text{const}$ can be achieved by adjusting R and ζ.

B. Ionization-Acceleration Region

Shown in Fig. 4 is the ionization-acceleration region, where the magnetic field is radial and has a uniform value of B_r. We assume that E equals U_d/L because the electric field outside this region is negligible, that is,

$$E = U_d/L \tag{1}$$

C. Main Results

Based on the assumptions, we can get the following results:

1) Equation (2) holds if $T_e(z/L) = \text{const}$, $\lambda/L = \text{const}$ and local geometric similarity.

$$n_n(z/L) \sim R^{\zeta-2}, \qquad n_e(z/L) \sim R^{\zeta-2}$$
$$n_i(z/L) \sim R^{\zeta-2} \tag{2}$$

Proof: According to the existing scaling theory, α is determined by the value of λ/L (Ref. 5), and so

$$\lambda/L = 1/n\sigma L = \text{const} \Rightarrow \alpha = \text{const} \tag{3}$$

Besides, σ is only the function of T_e (Ref. 5); thus,

$$T_e(z/L) = \text{const} \Rightarrow \sigma(z/L) = \text{const} \tag{4}$$

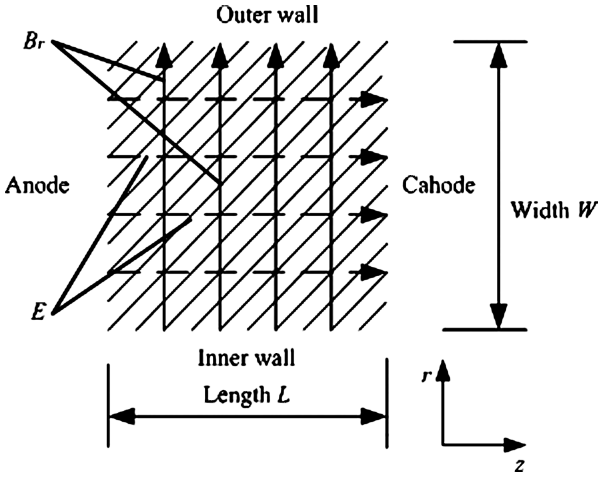

Fig. 4 Ionization-acceleration region.

Combining Eqs. (3) and (4) with $L \sim R^{2-\zeta}$, one can obtain Eq. (2).

2) Equation (5) holds if $U_d = \text{const}$, local geometric similarity, and T_n does not rise appreciably.

$$\dot{m} \sim R^{\zeta} \tag{5}$$

Proof: For SPT, $\dot{m}$ can be written as

$$\dot{m} = (n_{ie}u_{ie} + n_{ne}u_{ne})M\pi(R^2 - r^2) \tag{6}$$

Here, u_{ie} is assumed to be invariant if U_d keeps constant, that is,

$$U_d = \text{const} \Rightarrow u_{ie} = \text{const} \tag{7}$$

Considering $u_{ne} = \frac{1}{4}\sqrt{3kT_n/M}$ and T_n does not rise appreciably,[13,15] one can obtain

$$T_n = \text{const} \Rightarrow u_{ne} = \text{const} \tag{8}$$

Additionally, according to Eq. (2), one can obtain

$$n_{ne} \sim R^{\zeta-2}, \qquad n_{ie} \sim R^{\zeta-2} \tag{9}$$

Substituting Eqs. (7–9) and $r/R = \text{const}$ into Eq. (6) gives Eq. (5).

3) Equation (10) holds if $T_e(z/L) = \text{const}$, $\lambda/L = \text{const}$, and local geometric similarity.

$$B_r \sim R^{(\zeta-3)/2} \tag{10}$$

Proof: The movement of electron passing through the ionization-acceleration region with a radial B_r results in[14,16]

$$L \approx \sqrt{\frac{mU_d\nu_e}{eB_r^2\nu_i}} \Rightarrow B_r \approx \frac{1}{L}\sqrt{\frac{mU_d}{e}\frac{\nu_e}{\nu_i}} \tag{11}$$

Experimental data show[14]

$$\left.\begin{aligned} &\nu_e = \nu_{ei} + \nu_{ea} + \nu_{ew} \\ &\nu_{ew} \gg \nu_{ei} + \nu_{ea} \\ &\nu_{ew} \sim u_{et}/W \end{aligned}\right\} \Rightarrow \nu_e \sim u_{et}/W$$

or

$$\begin{cases} \nu_e = \nu_{ei} + \nu_{ea} + \nu_{ew} \\ \nu_{ew} \gg \nu_{ei} + \nu_{ea} \\ \nu_{ew} \sim u_{et}/W \end{cases} \Rightarrow \nu_e \sim u_{et}/W \tag{12}$$

Additionally, similar to chemical reaction rate, ν_i can be written as[17]

$$\nu_i = g_i/n_e = n_n\alpha_i\left(T_e^{0.5}\right) \tag{13}$$

Here, u_{et} and $\alpha_i(T_e^{0.5})$ are only the functions of T_e for special propellent,[17] then

$$T_e = \text{const} \Rightarrow \begin{cases} u_{et} = \text{const} \\ \alpha_i\left(T_e^{0.5}\right) = \text{const} \end{cases} \tag{14}$$

Substituting Eqs. (12) and (13) into Eq. (11) and recalling local geometric similarity, Eqs. (2) and (14), one can immediately obtain Eq. (10).

4) Equation (15) holds if $T_e(z/L) = \text{const}$, $\lambda/L = \text{const}$, $U_d = \text{const}$, and local geometric similarity.

$$j_d \sim R^{\zeta-2}, \qquad I_d \sim R^{\zeta}, \qquad P \sim R^{\zeta} \tag{15}$$

Proof: According to Ohm's law, one can get

$$j_e = \sigma_\perp E \tag{16}$$

It is well known that $\sigma_\perp = \sigma_0/1 + (\omega_e/\nu_e)^2$ and $\sigma_0 = n_e e^2/m\nu_e$. Because $\omega_e/\nu_e \gg 1$ and $\omega_e = eB_r/m$ in SPT,[17] then

$$\omega_e/\nu_e \gg 1 \Rightarrow \sigma_\perp(z/L) \approx n_e m\nu_e \Big/ B_r^2 \tag{17}$$

Substituting Eqs. (2), (10), and (12) into Eq. (17), one can obtain

$$\sigma_{\perp}(z/L) \approx \text{const} \tag{18}$$

Thus, combining Eq. (16) with Eq. (18), one can obtain

$$E \sim R^{\zeta-2} \Rightarrow j_{ee} \sim R^{\zeta-2} \tag{19}$$

Here $E \sim R^{\zeta-2}$ can be obtained from Eq. (1).

Additionally, because $j_{ie} = en_{ie}u_{ie}$, then

$$\begin{cases} n_{ie} \sim R^{\zeta-2} \\ u_{ie} = \text{const} \end{cases} \Rightarrow j_{ie} \sim R^{\zeta-2} \tag{20}$$

Besides,

$$j_d = j_{ee} + j_{ie}, \qquad I_d = j_d\pi(R^2 - r^2), \qquad P = U_d I_d$$

then

$$\begin{cases} j_{ee} \sim R^{\zeta-2} \\ j_{ie} \sim R^{\zeta-2} \\ U_d = \text{const} \end{cases} \Rightarrow \begin{cases} j_d \sim R^{\zeta-2} \\ I_d \sim R^{\zeta} \\ P \sim R^{\zeta} \end{cases} \tag{21}$$

5) Equation (22) holds if $T_e(z/L) = \text{const}$, $\lambda/L = \text{const}$, and local geometric similarity.

$$r_e \sim R^{(3-\zeta)/2}, \qquad \omega_e \sim R^{(\zeta-3)/2} \tag{22}$$

Proof: Because

$$r_e \sim T_e^{\frac{1}{2}} \Big/ B_r, \qquad \omega_e = eB_r/m$$

then[12]

$$B_r \sim R^{(\zeta-3)/2} \Rightarrow \begin{cases} r_e \sim R^{(3-\zeta)/2} \\ \omega_e \sim R^{(\zeta-3)/2} \end{cases} \tag{23}$$

6) Equation (24) holds if $T_e(z/L) = \text{const}$, $\lambda/L = \text{const}$, and local geometric similarity.

$$\beta \sim R^{(\zeta-1)/2} \tag{24}$$

Proof: Because $\beta = \omega_e/\nu_e$, then

$$\begin{cases} \omega_e \sim R^{(\zeta-3)/2} \\ \nu_e \sim R^{-1} \end{cases} \Rightarrow \beta \sim R^{(\zeta-1)/2} \tag{25}$$

Here, $\nu_e \sim R^{-1}$ can be obtained from Eqs. (12) and (14).

7) Equation (26) holds if $T_e(z/L) = \text{const}$, $\lambda/L = \text{const}$, and local geometric similarity.

$$u_d \sim R^{(\zeta-1)/2} \tag{26}$$

Proof: u_d equals E/B_r in the crossed electromagnetic field, then

$$\begin{cases} B_r \sim R^{(\zeta-3)/2} \\ E \sim R^{\zeta-2} \end{cases} \Rightarrow u_d \sim R^{(\zeta-1)/2} \tag{27}$$

8) Equation (28) holds if $T_e(z/L) = \text{const}$, $\lambda/L = \text{const}$, and local geometric similarity.

$$\mu_{e\perp} \sim R^{2-\zeta} \tag{28}$$

Proof: Because

$$\mu_{e\perp} \approx \mu_{e0}/(\omega_e/\nu_e)^2, \qquad \mu_{e0} = e/m\nu_e$$

then

$$\begin{cases} \omega_e \sim R^{(\zeta-3)/2} \\ \nu_e \sim R^{-1} \end{cases} \Rightarrow \mu_{e\perp} \sim R^{2-\zeta} \tag{29}$$

9) Equation (30) holds if $T_e(z/L) = \text{const}$, $\lambda/L = \text{const}$, $U_d = \text{const}$, local geometric similarity, and T_n does not rise appreciably.

$$T \sim R^{\zeta} \tag{30}$$

Proof: For SPT, $T = \dot{m}u_{ie}$, then

$$\begin{cases} \dot{m} \sim R^{\zeta} \\ u_{ie} = \text{const} \end{cases} \Rightarrow T \sim R^{\zeta} \tag{31}$$

IV. Comparison of Two Theories

It is presumed that $R^{2-\zeta}/L = \text{const}$ rather than $R/L = \text{const}$ is adopted in our proposed scaling theory, and this results in the differences between our proposed and the existing scaling theory, as shown in Table 3.

It is expected that ζ is larger than 0; otherwise, the power will decrease (increase) with the increasing (decreasing) of device sizes.

Shown in Figs. 5–7 are plots of calculated and measured results showing the dependence of power, mass flow rate, and thrust on SPT radius. The dotted, dash-dotted, solid, and broken lines correspond to the case when $\zeta = 1$, 1.5, 2, 2.5, respectively. The asterisks are experimental results. It is shown that the results from our proposed scaling theory agree well with the experimental results.

According to Eq. (2), $\zeta = 2$ can be a good choice if we want to maintain constant plasma density. Another character of $\zeta = 2$ is that the axial characteristic length can keep constant.

For lower powers, because $R^{2-\zeta}/L = \text{const}$ and $P \sim R^{\zeta}$, $0 < \zeta < 2$ should be satisfied to make the dimensions small. According to Eq. (2), plasma density will increase while the dimensions decrease, which leads to serious ion sputtering and low efficiency. $\zeta > 2$ can be a choice to alleviate the phenomena. For higher powers, the main concern is not to alleviate ion sputtering, but to improve $P/M_t g$ and $T/M_t g$, which can be achieved if ζ is larger than 2.

A. Improvement of Lower Powers

1. Reducing the Probability of Magnetic Saturation

Here, a model with power P is used to design a thruster with power $P^*(P^* < P)$. Φ can be roughly written as

$$\Phi \approx B_r\pi(r + R)L \tag{32}$$

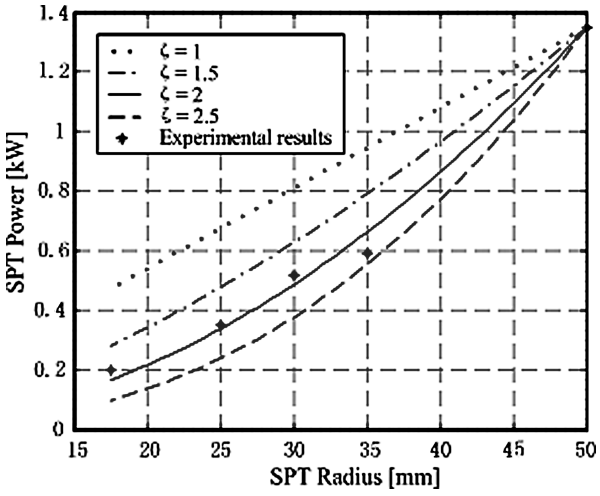

Fig. 5 Relationship between P and R.

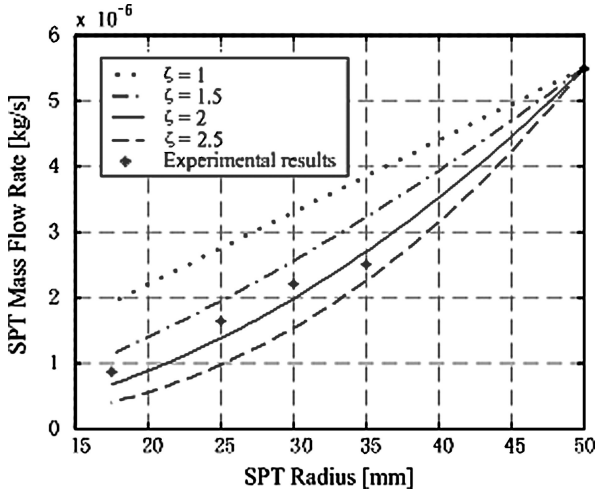

Fig. 6 Relationship between $\dot{m}$ and R.

Table 3 Main differences between two theories

Theory	n	$\dot{m}$	P	I	j_d	B_r	E	u_d	ω_e	r_e	μ_e	T
Existing	$\sim R^{-1}$	$\sim R$	$\sim R$	$\sim R$	$\sim R^{-1}$	$\sim R^{-1}$	$\sim R^{-1}$	const	$\sim R^{-1}$	$\sim R$	$\sim R$	$\sim R$
Proposed	$\sim R^{\zeta-2}$	$\sim R^{\zeta}$	$\sim R^{\zeta}$	$\sim R^{\zeta}$	$\sim R^{\zeta-2}$	$\sim R^{(\zeta-3)/2}$	$\sim R^{\zeta-2}$	$\sim R^{(\zeta-1)/2}$	$\sim R^{(\zeta-3)/2}$	$\sim R^{(3-\zeta)/2}$	$\sim R^{2-\zeta}$	$\sim R^{\zeta}$

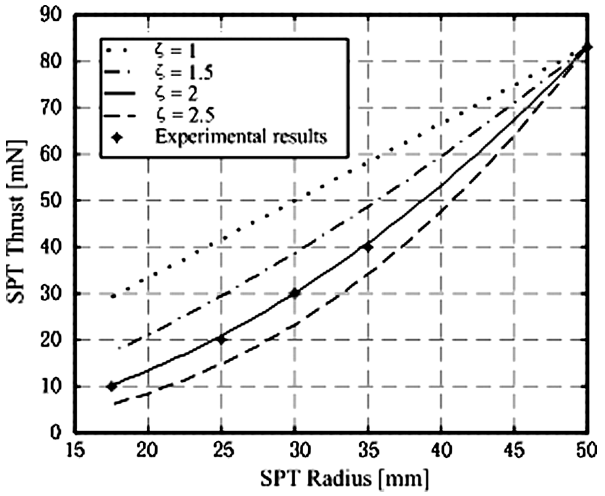

Fig. 7 Relationship between T and R.

Then the magnetic field induction in magnetic core is

$$B_i = \Phi/\pi R_i^2 \tag{33}$$

If $R_i/R = \text{const}$, then

$$B_{i1}/B_i \sim P/P^* \tag{34}$$

Equation (34) shows that with small values of P^* one can obtain magnetic core saturation. In other words, it is impossible to maintain optimal magnetic field topology and induction under reduced P^* values, and this will inevitably reduce the efficiency.

According to our proposed scaling theory, one can get

$$B_{i2}/B_i \sim (P/P^*)^{(\zeta+1)/2\zeta} \tag{35}$$

Then, if $\zeta > 1$, B_{i2} will be smaller than B_{i1}. It implies that the probability of magnetic saturation can be reduced if ζ is properly set. To avoid magnetic saturation, B_{i2} should be smaller than B_s, then

$$P^* > P(B_s/B_i)^{-2\zeta/(1+\zeta)} \tag{36}$$

2. Alleviating Ion Sputtering

Ion sputtering will be aggravated for narrower channel width and higher ion density. Combining $W_2 \sim R_2$, $n_{i2} \sim R_2^{\zeta-2}$, and $P^* \sim R_2^{\zeta}$ in our proposed scaling theory with $W_1 \sim R_1$, $n_{i1} \sim R_1^{-1}$, and $P^* \sim R_1$ in the existing scaling theory, one can get

$$\frac{W_2}{W_1} \sim \left(\frac{P^*}{P}\right)^{(1-\zeta)/\zeta}, \qquad \frac{n_{i2}}{n_{i1}} \sim \left(\frac{P^*}{P}\right)^{2-2/\zeta} \tag{37}$$

According to Eq. (37), the performance of lower powers can be improved if ζ is properly set. For example, if $\zeta > 1$, our proposed theory can decrease the probability of ion collision with wall and then alleviate ion sputtering because $W_2 > W_1$ and $n_{i2} < n_{i1}$.

B. Improvement of Higher Powers

Here, we design a thruster with power $P^*(P^* > P)$. And we presume that $M_t \sim R^2 l$ and $l \sim L$. Thus, according to the existing scaling theory, one can get

$$\frac{P^*/M_{t1}g}{P/M_t g} \sim \left(\frac{P}{P^*}\right)^2, \qquad \frac{T_1/M_{t1}g}{T/M_t g} \sim \left(\frac{P}{P^*}\right)^2 \tag{38}$$

Equation (38) shows that the larger the values of P^*, the smaller the values of $P^*/M_{t1}g$ and $T_1/M_{t1}g$. Thus the performance of higher powers is difficult to improve as a result of large dimensions and weights.

However, according to our proposed scaling theory, one can get

$$\frac{P^*/M_{t2}g}{P/M_t g} \sim \left(\frac{P^*}{P}\right)^{2-4/\zeta}, \qquad \frac{T_2/M_{t2}g}{T/M_t g} \sim \left(\frac{P^*}{P}\right)^{2-4/\zeta} \tag{39}$$

According to Eq. (39), if $\zeta > 2$, $P/M_t g$ of the desired thruster will be larger than that of the model, and so does $T/M_t g$.

V. Conclusions

Compared with the existing scaling theory, our proposed one can enlarge the degrees of freedom in the thruster design. When $\zeta = 2$, P, $\dot{m}$, and T are respectively proportional to R^2, which agrees well with the experimental results, and the plasma density in the desired thruster is as the same as that in the model. $\zeta > 2$ can be a choice for reducing the probability of magnetic saturation and alleviating ion sputtering for lower powers, and also can be a choice for improving the power-to-weight ratio and thrust-to-weight ratio for higher powers.

References

[1]Szabo, J. J., and Pollard, J. E., "A Laboratory-Scale Hall Thruster," AIAA Paper 95-2926, July 1995.

[2]Perot, C., Gascon, N., Bechu, S., Lasgorceix, P., Dudeck, M., Garrigues, L., and Boeuf, J. P., "Characterization of a Laboratory Hall Thruster with Electrical Probes and Comparisons with a 2D Hybrid PIC-MCC Model," AIAA Paper 99-2716, June 1999.

[3]Haas, J. M., Gulczinski, F. S., III, and Gallimore, A. D., "Performance Characteristics of a 5kW Laboratory Hall Thruster," AIAA Paper 97-3503, July 1998.

[4]Raitses, Y., and Fisch, N. J., "Parametric Investigations of Non-Conventional Hall Thruster," Princeton Univ., PPPL-3534, NJ, Jan. 2001.

[5]Khayms, V., and Martinez-Sanchez, M., "Design of a Miniaturized Hall Thruster for Microsatellites," AIAA Paper 96-329, July 1996.

[6]Kim, V., "Main Physical Features and Processes Determining the Performance of Stationary Plasma Thruster," *Journal of Propulsion and Power*, Vol. 14, No. 5, 1998, pp. 736–743.

[7]Gorshkov, O., "Russian Electric Propulsion Thruster Today," *Russian Space News*, Vol. 9, No. 7, 1999, pp. 5–11.

[8]Morozov, A. I., and Melikov, I. A., "The Process Scaling in the Plasma Accelerator with Closed Electron Drift Under the Condition of Ionization," *Journal of Technical Physics*, Vol. XLIV, No. 5, 1974, pp. 544–548 (in Russian).

[9]Bugrova, A. I., Maslennikov, N., and Morozov, A. I., "Similarity Laws for the Global Properties of a Hall Accelerator," *Journal of Technical Physics*, Vol. 61, No. 6, 1991, pp. 45–51 (in Russian).

[10]Bugrova, A. I., Lipatov, A. S., Morozov, A. I., and Solomatina, L. V., "Global Characteristics of an ATON Stationary Plasma Thruster Operating with Krypton and Xenon," *Plasma Physics Reports*, Vol. 28, No. 6, 2002, pp. 1032–1037.

[11]Bugrova, A. I., Lipatov, A. S., and Morozov, A. I., "On a Similarity Criterion for Plasma Accelerators of the Stationary Plasma Thruster Type," *Technical Physics Letters*, Vol. 28, No. 10, 2002, pp. 821–823.

[12]Hargus, W. A., Jr., and Cappelli, M. A., "Development of a Linear Hall Thruster," AIAA Paper 98-3336, July 1998.

[13]Hargus, W. A., Jr., "Investigation of the Plasma Acceleration Mechanism Within a Coaxial Hall Thruster," Stanford Univ., TSD-130, CA, March 2001.

[14]Kim, V., Kozlov, V., Lazurenko, A., Popov, G., and Skrulnikov, A., "Development and Characterization of Small SPT," AIAA Paper 98-3335, July 1998.

[15]Komurasaki, K., Mikami, K., and Kusamoto, D., "Channel Length and Thruster Performance of Hall Thrusters," AIAA Paper 96-3194, July 1996.

[16]Zhurin, V. V., Kaufman, H. R., and Robinson, R. S., "Physics of Closed Drift Thrusters," *Plasma Sources Science and Technology*, Vol. 8, No. 1, 1999, pp. 1–20.

[17]Schmidt, D. P., Meezan, N. B., Hargus, W. A., Jr., and Cappelli, M. A., "Operating Characteristics of a Linear Hall Thruster with an Open Electron-Drift," AIAA Paper 99-2569, June 1999.